EFFECT OF PROCESS PARAMETERS ON MECHANICAL PROPERTIES OF THERMOPLASTIC COMPOSITE RINGS MANUFACTURED BY LASER-ASSISTED FIBER PLACEMENT

Eimanlou, Mehran and Hojjati, Mehdi
Mechanical and Industrial Engineering, Concordia Center for Composites,
Concordia University, Montreal, Canada
Corresponding author (mehran.eimanlou@gmail.com)

Keywords: *Laser-assisted Processing, Thermoplastics, Composite Manufacturing*

ABSTRACT

The competitive advantage of an automated, true out-of-autoclave thermoplastic composite manufacturing process is realized. Decades of research has been directed toward enhancing technologies and processes such as the automated fiber placement (AFP). The latest technological advancement in the AFP process is the introduction of continuous-wave high power fiber lasers. Together with development of thermoplastic material systems, it is now possible to in-situ consolidate parts at efficient rates with promising quality. A ring manufacturing setup capable of in-situ consolidation of thermoplastic composite tape using a 2kW continuous fiber laser is developed. A beam shaping lens is used to –ideally- transform a Gaussian beam with a conical profile to a square top-hatted beam with uniform intensity profile at the working distance. The measurement of 2D profile of the beam at various axial locations shows that the beam intensity and uniformity is very sensitive to axial distance. An experimental study is carried out to investigate the quality of the parts manufactured using different material and heating systems. Both laser-assisted (LA), and hot-gas-torch (HGT) heating systems were used. For laser processing, lay-up speed, and laser power are selected as variables whereas the optimum condition is constrained by interlaminar shear strength ILSS measured using short beam shear test. The result shows that the quality of the tows is important in the final part quality. Also the ILSS results indicate that the laser can produce good quality parts at the higher processing speed.

1 INTRODUCTION

Today automated placement of composite has found extensive application in aerospace and aeronautic industry with automotive catching up to the race. The demand for low cost, highly efficient manufacturing process is rising as cost competitiveness becomes an advantage and production rates deem to increase. The benefits of fully automated placement technologies have been realized. A pair of robots moving in synchronized manner meticulously places a narrow tape on a convex mandrel. Many aerospace OEMs are using fiber placement technology for their new products development and manufacturing including Bombardier Aerospace. One strip at a time, the rear pressure bulkhead of the CSeries fuselage is being crafted. Design engineers take advantage of the anisotropic behavior of composites on the highly curved dome shape to deliver yet lighter components. Through the use of AFP, higher productivity and lower manufacturing costs have been reached. However the final thermoset based part must be bagged and cured in autoclave. The use of autoclaves still remains as the major bottleneck to the manufacturing process. Hence high performance thermoplastic based composite tapes are developed to eliminate the need for curing. Thermoplastic prepreg tapes are capable of being welded, recycled and have infinite shelf life. Higher process rates are also feasible with new Laser heating systems and high performance PEEK materials which are least sensitive to the cooling rates [1].

A major pullback to the technology however has been low production rates and below autoclave level part quality. To address the low production rate high power fiber laser heating have been developed to replace hot-gas-torch. The continuous wave high power fiber lasers are a more uniform and very efficient source of heat [2]. The major limitation to hot-gas-torch is that the surface of the tape being processed is heated through convection. Higher process rate means blast of even hotter gas to the surface of the tape. This typically results in degradation of the thermoplastic matrix. In laser heating however the transfer of heat is through radiation. The radiance is at first fully absorbed by the fibers as the matrix is transparent to 1064 nm near-infrared (NIR) wavelength. The surrounding matrix is then heated through conduction by adjacent fibers. This allows for minimal degradation at increased heating rates.

Recent work reported placement rates as much as 400mm/s and near autoclave properties for flat plates [3]. The drastic increase in placement rate is mostly become possible with the use of large conformable silicone rollers which extend the time material spends under pressure and therefore enhance degree of intimate contact. However a major challenge remains to attain aerospace standard quality for complex parts with small radius of curvature. For example, a cylindrical tailboom was manufactured using HGT AFP system with a small 6.35 mm (1/2 in) diameter steel roller to study the feasibility of the process. Less than 75 mm/s (3 in/s) placement rate was used during this process to obtain high quality parts [4]. The present work is an extension to earlier optimization study carried out by the authors [5]. The objective of the study is to investigate the influence of heating and material system in the placement process.

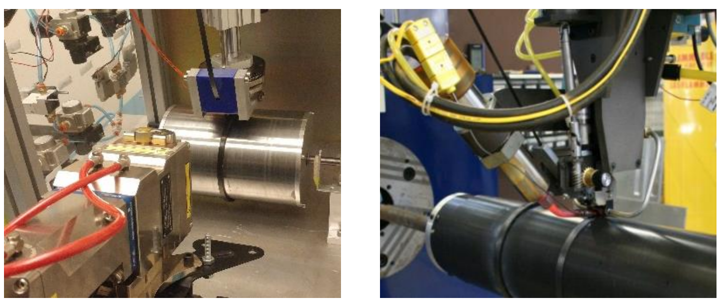

Figure 1: Laser-Assisted setup (left), Hot-Gas-Torch setup (right) [4]

2 Experimental Investigation

2.1 Ring Manufacturing Apparatus Development

The experimental work presented henceforth initiated with development of a fiber placement setup. The ring manufacturing setup had to be capable of in-situ consolidating thermoplastic composite rings with a 2 kW Nd-Yag fiber laser. Hence, functionality and safety were the major requirement of the design. The 3D model of the set-up is shown in Figure 2. It consists of three main components: a pneumatic actuator to apply compaction force, a servo motor to adjust the placement rate, and a set of optics which are used to manipulate Gaussian laser beam and output a focused, top-hatted, square beam. Other components include a pneumatic clutch, a multi-axial load cell, a microcontroller, a fume extractor, and a set of cameras. They are used respectively to keep tension in the tape, measure the compaction force, regulate the switches, ventilate, and filter smoke, and monitor the process.

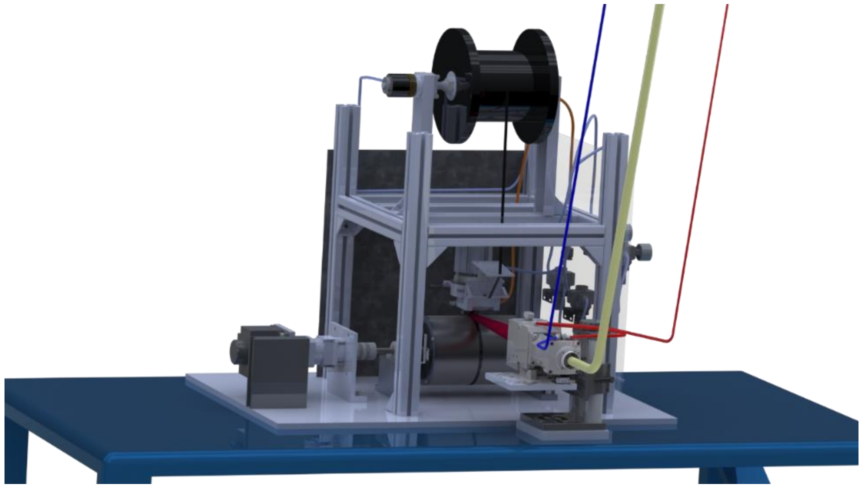

Figure 2: In-house developed laser-assisted ring manufacturing apparatus

Prototypes of each major components were built and tested concurrently during the development phase to assure functionality, and avoid scrap and rework. Concurrent development also allowed for involvement of all parties concerned with the design, and the safety of the project at every stage. To roll out the risks associated with the laser exposure, the nominal hazard zone (NHZ) –area around a laser beam where potential exposure exceeds a certain limit- is contained and the process is monitored using infrared cameras. The pneumatic valves, and the electric motor driver are remotely controlled from the work station outside the NHZ.

a.

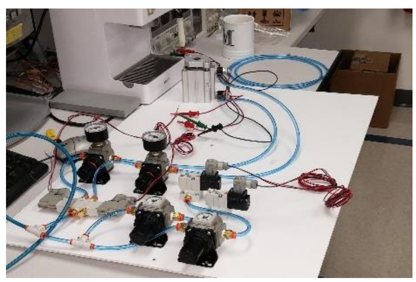

b.

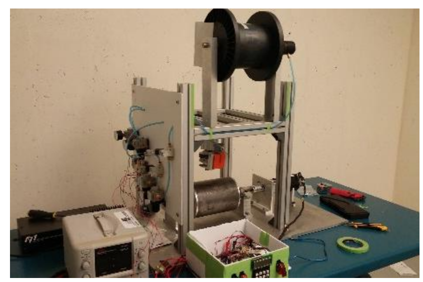

c.

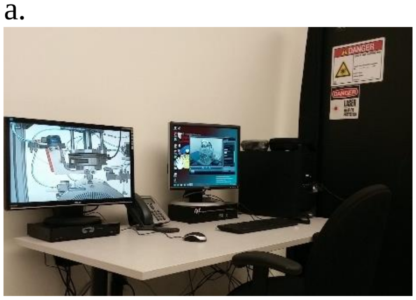

d.

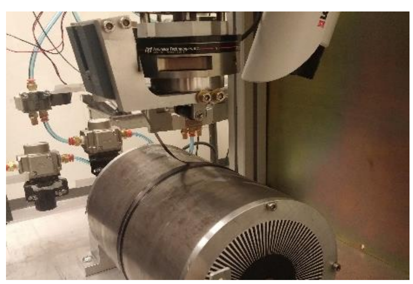

e.

f.

Figure 3: a. geared motor and steel mandrel; b. pneumatic actuator and regulators; c. testing prototype; d. process monitoring from workstation; e. in-situ consolidated carbon fiber reinforced PEEK ring; f. complete setup

Additionally the operator zone is divided by aluminum barriers. Figure 3 demonstrates the development of the apparatus and its current configuration.

2.2 Diode Laser Beam Delivery

The diode beam leaving the optical cable is a highly divergent beam with a small diameter of 50 µm. To process the composite tape however, the beam must be collimated, focused, and widened to at least match the width of the tape being processed. Beam delivery is an important factor in process optimization as it highly affects part quality.

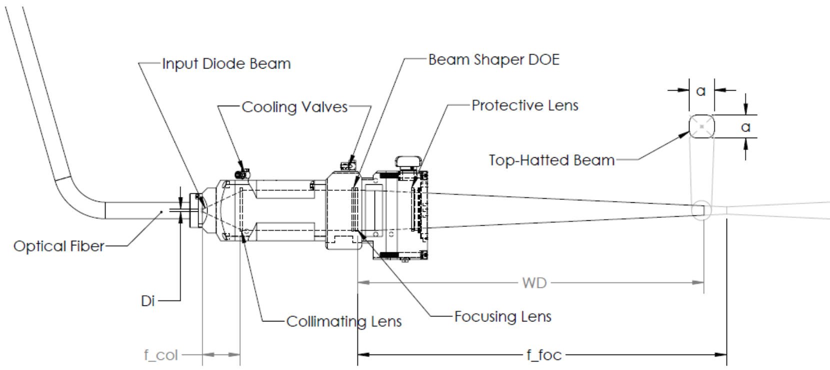

Figure 4: Collimating and beam shaping module for the Ring Manufacturing setup

An IPG welding head with water cooling is used here to deliver the diode beam as shown in 4. For the current setup a working distance (WD) of 300mm and a square beam of 6.5mm is selected. A beam shaping lens is used to – ideally- transform a Gaussian beam with a conical profile to a sharp edged, top-hatted, uniform intensity profile at the working distance. The ideal profile of a square top-hatted beam is shown in Figure 5 below. However the real output of the beam at the WD may deviate from the ideal profile depending on the design of the optics. The shape, uniformity and sensitivity of the beam characterize the beam delivery.

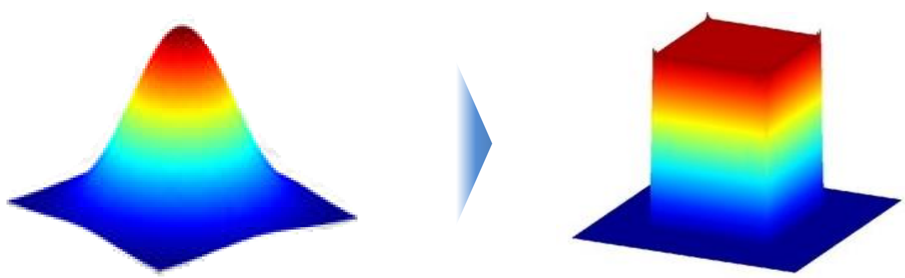

Figure 5: Transformation of a Gaussian beam (left) to top-hatted beam (right)

To measure and characterize the beam intensity and uniformity, a ceramic IR conversion screen rated for radiation of up to $3kW/cm^2$ and a thermal camera are used to capture the 2D radiance profile of the beam at locations close, and away from the working distance. The surface temperature of the conversion screen is recorded for 10 seconds of continuous emission. The surface temperature reaches a steady state during this time. The images of the radiance profile at various axial distances from the nip point are presented in the Figure 6 below.

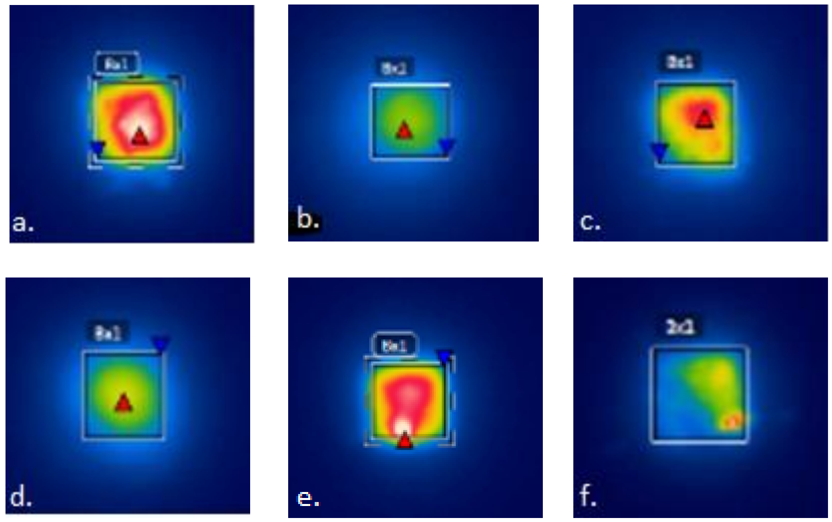

Figure6: Conversion screen surface temperature at various distances from WD: a) at WD, b) -25.4mm (-1 in), c) +19.05 mm (+0.75in), d) +25.4 mm (+1 in) e) 50.8 mm (+2in), f) +76.2 mm (+3in)

The absolute temperatures tabulated below are used for comparison of the radiance profiles and are not the real surface temperatures of the ceramic screen. The percentage difference in the average temperature shows the reduction in average radiance flux and therefore laser effectiveness η_n:

$$\eta_n = \frac{P_{eff}}{P_{in}} \tag{1}$$

Table I: Temperatures recorded for differnt radiance profiles

ID	Hot Spot Temp. [°C]	Cold Spot Temp. [°C]	Average Temp. [°C]	Delta Ave. Temp. [%]	Laser Effectiveness $\boldsymbol{\eta_n}$
a.	150	64	115	0	0.95
b.	90	52	77	-33	0.63
c.	134	56	97	-16	0.80
d.	98	56	80	-30	0.66
e.	177	60	114	0	0.95
f.	136	44	66	-43	0.54

Assuming 5% losses through optics, η_n is calculated for the radiance profiles shown in Table 1. It is noted that the shape and intensity of the profile is sensitive to variation from the working distance. Also that the beam at the nip point is off-focused and there are two distinct locations at which the radiance is near-uniform: one behind the beam waist, where $w(z) = w_o$ and one after as shown in Figure 7. The intensity fades away as the distance increases from the WD. This introduces a limitation on the size of the beam. A large rectangular shaped beam is often used to preheat the tape and the substrate to enhance bonding. Better bonding is achieved due to the larger wetted area which increases the thermal efficiency. Thermal efficiency is the ratio of the amount of heat required to raise the matrix temperature above T_m to the total amount of heat delivered:

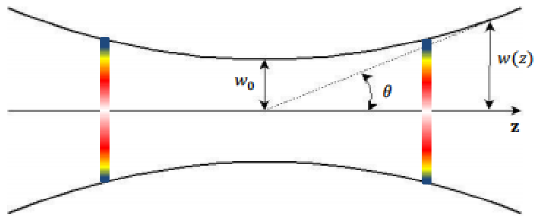

Figure 7: Gaussian beam width as a function of axial distance z. The two gradient collored lines indicate two distinct focused beam spots for the ring manufactuirng setup

$$\eta_{th} = \frac{vS_m C_m}{P_{eff}} \tag{2}$$

whereas v is the placement rate; S is the cross sectional area of the molten matrix; and C is the heat content per unit volume of the molten matrix [6]. However the larger the beam, the larger will be the wetted area away from the WD, and the weaker will be the area averaged beam intensity as a result. The variation in intensity follows a Super-Gaussian radiance intensity:

$$I(P, r, z, n) = \frac{P_{in}}{\frac{\pi}{2}\omega^2(z)} e^{-2(\frac{r}{\omega(z)})^n} \tag{3}$$

where P_{in} is the Gaussian beam power; ω is the beam radius; z is the axial distance from the beam waist; r is the beam radial location; and n is the order of a Super-Gaussian beam. As the order n increases the Gaussian beam transforms toward a flat, top-hatted beam with sharp edges [7]. For on-axis intensity:

$$I_{axis}(z) = \frac{P_{in}}{\frac{\pi}{2}\omega^2(z)} \tag{4}$$

where $\omega(z)$ *is the beam waist at any axial location*:

$$\omega(z) = \omega_o \sqrt{1 + (\frac{z}{z_R})^2} \tag{5}$$

By knowing $I_{axis}(z)$ and I_o the laser effectiveness η_n can be measured at any axial distance. Effectiveness can be improved by increasing the angle of the incoming tape, away from the substrate. However this is achieved at the cost of reduction in the wetted area. An alternative approach is to reduce the sensitivity of the beam. The sensitivity of the beam can be characterized by Rayleigh length, z_R which is the axial distance from the waist to where the beam width is doubled:

$$z_R = \frac{\pi {\omega_o}^2}{M^2 \lambda} \tag{6}$$

whereas ω_o is the beam waist, λ is the beam wavelength, and M^2 factor is the deviation of the laser beam from a perfect Gaussian beam. The profile is less sensitive to axial distance variation for a large Rayleigh length. To maximize z_R the beam waist is to be maximized and M^2 factor to be minimized. This is achieved by having a larger input beam diameter D_i for the same magnification MP:

$$\omega_o = MP \times D_i = \frac{f_{foc}}{f_{col}} D_i \tag{7}$$

whereas f_{foc} and f_{col} are the focal length of the focusing lens, and of the collimating lens respectively. Lastly the divergent angle θ as shown in Figure 7 is:

$$\theta = \frac{M^2 \lambda}{\pi \omega_o} \tag{7}$$

The current laser setup has an input diameter of 50 μm, magnification of 4.2 and M^2 factor of 1.11 resulting in a long Rayleigh range of 107mm. The sensitivity can be further improved by increasing the magnification power.

2.3 Laser-Assisted vs. Hot-Gas-Torch: Comparison of Mechanical Properties at Optimum Condition

The current study is based on the earlier optimization study carried out by the authors to determine the effect of process parameters on inter-laminar quality of rings made using laser-assisted setup. Numerous variables were identified to have an effect on the outcome of the laser-assisted placement to various extents as listed below.

Table II: List of factors affecting the outcome of the laser-assisted placement process

Parameters Affecting Process Outcome			
F	Compaction Force	T_s	Substrate Temperature
D_r	Roller Diameter	Y	Beam Profile Uniformity
k_r	Roller Thermal Conductivity	I	Beam Intensity
T_r	Roller NIP Temperature	W	Beam Width
h	Heat Transfer Coefficient	β	Beam Angle
T_m	Mandrel Temperature	Bi	Beam Position Bias
k_m	Mandrel Thermal Conductivity	T	Tape Tension
D_m	Mandrel Curvature	V_f	Tape Void Fraction
S	Compaction Surface Area	X	Tape Surface Roughness
N	Placement Rate	α	Tape Angle

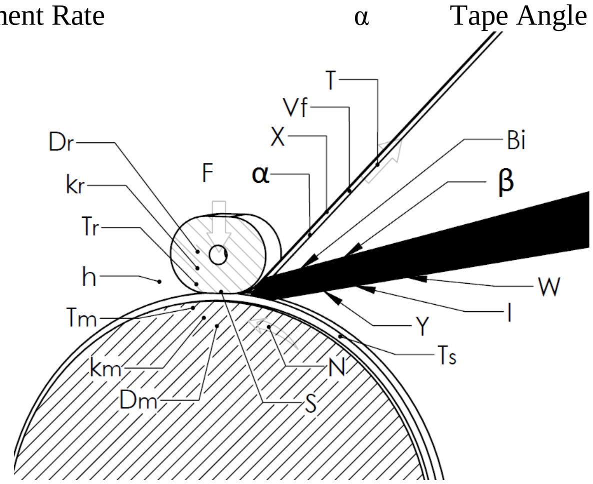

Figure 8: Schematic of laser-assisted process parameters

A DOE experiment was designed to efficiently investigate some of the parameters that deemed to be the most influential. The three selected parameters were namely, A: placement rate, B: laser power, and C: compaction force. Based on the result of the SBS test on 48 rings and more than 200 samples it was determined that compaction force, beyond 135 N has the least effect on the bond quality relative to placement rate, and laser power. Analysis of Variance was performed to calculate the relative influence of parameters for 95% confidence level [5]:

A = 86.3% B = 6.2% C = 0.7% Error = 6.8%

whereas the error term represented experimental error, noise factor, and controllable factors which were not considered in the experiment. An attempt is therefore made to investigate new parameters that were excluded from the study and may have had significant influence on the process outcome.

Based on previous practice it was known that any two material systems do not exhibit the same performance under similar HGT process conditions. Therefore the SBS of the two materials A) TenCate Cetex® TC1200 AS4/PEEK, and B)AS4/APC2 CYTEC are compared at their optimum condition. Twenty plies, 6.35 mm (¼ inch) wide, carbon fiber thermoplastic rings are made using two different AFP systems: CONCOM's Automated Dynamics hot-gas-torch end-effector, and the laser-assisted ring manufacturing setup. The rings made using HGT are processed at speed of 76 mm/s (3 in/s). The ones made using fiber laser setup are processed at the placement rate of 115mm/s (4.6 in/s). A constant compaction force of 400N (90lbf) is applied for all the trials. SBS test is carried out according to ASTM standard D2344M. The force versus displacement data is recorded and plotted by Hoskin Scientific Apparatus. The first maximum load is recorded and the ILSS is calculated as follows:

$$F^{SBS} = 0.75 \times \frac{P_m}{b \times t} \tag{9}$$

whereas P_m is the maximum load, b is the specimen width, and t is the specimen thickness. To prepare the samples the sides of the processed ring is first sanded to obtain a flat, parallel edge. A jig is then used to cut few specimens from random locations of the ring. Two flat blocks support the curved specimen with 12 mm spacing, placed equidistance with respect to the center of the loading nose. The loading nose, 6mm in diameter, is dropped at a constant speed of 1mm/min. A 5 kN load cell measures the applied force without any noticeable noise. A list of experimental trials and their associated ILSS results are tabulated below:

Table 3: Rings manufactured using HGT and laser source heating

Trial #	Material ID	Heating Source	Placement Rate [mm/s]	Laser Power [W]	ILSS [MPa]	Standard Deviation	CV %
1	B	Laser	115	240	35.4	0.91	2.58
2	B	Laser	115	245	42.8	1.67	3.89
3	B	Laser	115	250	40.9	1.27	3.10
4	B	Laser	115	255	40.3	2.30	5.70
5	B	Laser	115	260	44.9	1.68	3.75
6	B	Laser	115	265	40.3	2.20	5.47
7	B	Laser	115	258	45.4	2.21	4.87
8	B	Laser	115	262	39.2	0.98	2.49
9	A	HGT	76	NA	27.7	2.86	10.3
10	B	HGT	76	NA	45.4	2.99	6.57
11	A	Laser	115	255	42.2	1.6	3.80

It is noted that material "A" and "B" exhibit similar performance when laser heating source is used. Both material reach optimum ILSS for the laser power of 255-260 W. Material "B" however shows 7.6% improvement compared to material "A". A notable difference between the two materials is their surface roughness. It is believed that a higher degree of intimate contact and hence better bonding is achieved due to the higher surface roughness of material "B" compared to "A". Also tape "B" has a resin rich and a fiber rich surface. During the placement process the dry side of the tape is placed to face the roller while the resin rich side faces the substrate. This is because of the practical limitation of the process. At high heating rates, as the surface temperature of the roller increases, the tape tends to stick to the roller and peel away from the substrate. The dry side of the tape resists bonding to the surface of the roller and therefore allows material “B” to be processed at higher heating rates. This limitation is emphasized when dealing with HGT process. Hence it is the reason for material “A” exhibiting low ILSS at trial 9 where the tape bonded to the roller and was peeled off the substrate surface. The result also indicates lower deviation from population mean for specimen made using fiber laser. Less variation is also noted in plots of stiffness as shown in figure below. This could be mainly due to steady, uniform delivery of heat through fiber laser as opposed to unsteady blast of hot gas through a nozzle. However more data is required to confirm this result.

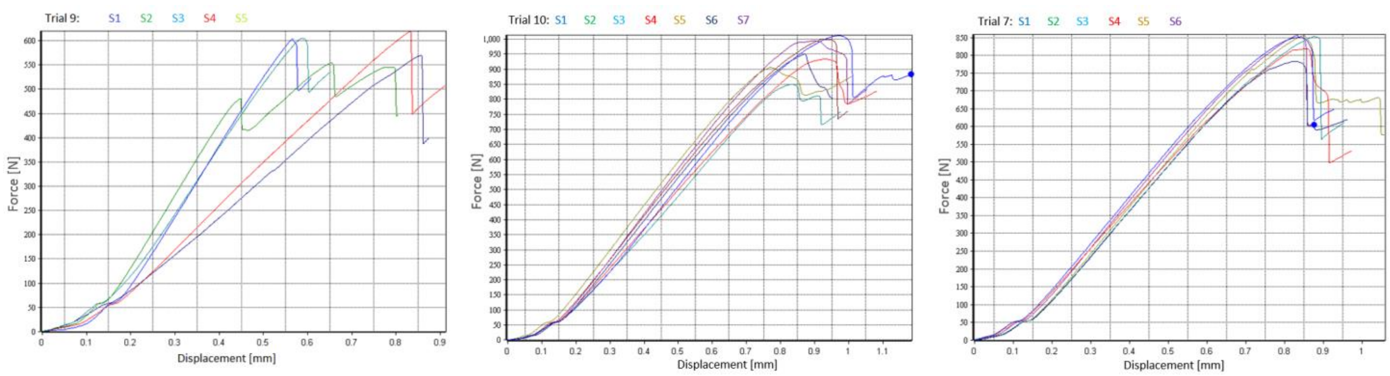

Figure 9: left to right: Trail 9: Material “A” processed with HGT, Trail 10: Material "B" processed with HGT, Trial 7: Material “B” Processed with Fiber Laser at optimum condition

Lastly it is noted that at the optimum condition, trial 7, the SBS test result of material “B” processed using fiber laser is matched to the SBS results of material “B” processed using HGT at trial 10, . However material “B” is processed at 50% higher rate using fiber laser heating compared to HGT. Since heating system was the only variable of the study, it is fair to say that fiber laser heating is at least 50% more efficient compared to HGT.

3 Conclusion

Experimental investigation has been successfully conducted with the in-house laser-assisted ring manufacturing setup. Based on the previous optimization work performed, a new study is carried out to assess the effect of different material and heating systems in fiber placement process. It is shown that the process is sensitive to beam quality and intensity. Therefore for a wide rectangular beam a uniform top-hatted beam with high Rayleigh range and magnification power is required to provide effective heating. Experimental result indicates that for a tow material with higher surface roughness, higher consolidation can be obtained. That is due to the higher degree of intimate contact and therefore enhanced bonding. Lastly, for the same placement setup in terms of productivity, the laser heating is shown to be 50% more efficient than HGT heating system.

4 References

[1] C.M.Pistor, S.I. Guceri, Crystallinity of On-Line Consolidated Thermoplastic Composites, Chicago: Journal of Composite Materials, Vol. 33, No. 4, 1999.

[2] S. R., Thermoplastic tape placement process - In situ consolidation is reachable, Plastic, Rubber and Composites. 38(9-10): 379-386, 2009.

[3] CM.J. Stokes-Griffin, P. Compston, The effect of processing temperature and placement rate on the short beam strength of

carbon-fibre-PEEK manufactured using a laser tape placement process, Composite Part A: Applied Science and Manufacturing. 78:247-283., 2015.

[4] X. Ciao, Determination of process parameters for the manufacturing of thermoplastic composite cones using automated fiber placement, Montreal: Concordia University Department of Mechnaical and Indsutreial Engineering, 2012.

[5] M. Eimanlou, M. Hojjati, "Automated Fiber Placement of Thermoplastic Composite Using Fiber Lasers," in *Proceedings 3rd International Symposium on Automated Composites Manufacturing*, Montreal, 2017.

[6] Grigoruants, Basics of Laser Material Processing, Moscow: Mir Publishers, 1994.

[7] O. Willstrand, "Intensity distribution conversion from Gaussian to Top-Hat in a single-mode fiber connector," Lund University, Lund, Sweden, 2013.